Functional interconnectivity between the globus pallidus and the subthalamic nucleus in the mouse brain slice

K. C. Loucif[1], C. L. Wilson[1,2], R. Baig[1], M. G. Lacey[2] and I. M. Stanford[1]

[1] *School of Life and Health Sciences, Aston University, Birmingham B4 7ET, UK*
[2] *Division of Neuroscience, The Medical School, University of Birmingham, Edgbaston, Birmingham B15 2TT, UK*

In accordance with its central role in basal ganglia circuitry, changes in the rate of action potential firing and pattern of activity in the globus pallidus (GP)–subthalamic nucleus (STN) network are apparent in movement disorders. In this study we have developed a mouse brain slice preparation that maintains the functional connectivity between the GP and STN in order to assess its role in shaping and modulating bursting activity promoted by pharmacological manipulations. Fibre-tract tracing studies indicated that a parasagittal slice cut 20 deg to the midline best preserved connectivity between the GP and the STN. IPSCs and EPSCs elicited by electrical stimulation confirmed connectivity from GP to STN in 44/59 slices and from STN to GP in 22/33 slices, respectively. In control slices, 74/76 (97%) of STN cells fired tonically at a rate of 10.3 ± 1.3 Hz. This rate and pattern of single spiking activity was unaffected by bath application of the $GABA_A$ antagonist picrotoxin (50 μM, $n = 9$) or the glutamate receptor antagonist (6-cyano-7-nitroquinoxaline-2, 3-dione (CNQX) 10 μM, $n = 8$). Bursting activity in STN neurones could be induced pharmacologically by application of NMDA alone (20 μM, 3/18 cells, 17%) but was more robust if NMDA was applied in conjunction with apamin (20–100 nM, 34/77 cells, 44%). Once again, neither picrotoxin (50 μM, $n = 5$) nor CNQX (10 μM, $n = 5$) had any effect on the frequency or pattern of the STN neurone activity while paired STN and GP recordings of tonic and bursting activity show no evidence of coherent activity. Thus, in a mouse brain slice preparation where functional GP–STN connectivity is preserved, no regenerative synaptically mediated activity indicative of a dynamic network is evident, either in the resting state or when neuronal bursting in both the GP and STN is generated by application of NMDA/apamin. This difference from the brain in Parkinson's disease may be attributed either to insufficient preservation of cortico-striato-pallidal or cortico-subthalamic circuitry, and/or an essential requirement for adaptive changes resulting from dopamine depletion for the expression of network activity within this tissue complex.

(Resubmitted 29 June 2005; accepted 14 July 2005; first published online 21 July 2005)
Corresponding author Ian M. Stanford: School of Life and Health Sciences, Aston University, Birmingham B4 7ET, UK.
Email: i.m.stanford@aston.ac.uk

During dopamine depletion in idiopathic and animal models of Parkinson's disease, overactivity of the indirect pathway of the basal ganglia, of which the globus pallidus (GP) and subthalamic nucleus (STN) are a part, leads to the excessive inhibition of the thalamo-cortical motor loop thus promoting akinesia and rigidity (Albin *et al.* 1989; DeLong, 1990). This pathophysiology is accompanied by, and indeed may be a consequence of, increases in the frequency of burst firing and synchronization of neuronal activity within GP–STN networks. This activity, which has been correlated with muscle tremor (Filion & Tremblay, 1991; Bergman *et al.* 1994; Magnin *et al.* 2002), may be reversed in animal models of, and patients with, Parkinson's disease by dopamine replacement therapy (Bergman *et al.* 1994; Heimer *et al.* 2002; Levy *et al.* 2002).

In vivo experiments have indicated that rhythmic activity in GP and STN neurones can be driven by the cortex (Magill *et al.* 2000), with dopamine depletion rendering the system more sensitive to rhythmical cortical input (Magill *et al.* 2001). However, using an organotypic culture preparation, Plenz & Kitai (1999) proposed that the GP and STN constitute a central pacemaker responsible for oscillatory activity. In these experiments, brief applications of GABA (to mimic pallidal synaptic input) were able to promote burst firing in the STN, through the de-inactivation of a low-threshold calcium conductance, while STN activity reverted to tonic firing once pallidal input was disconnected (Plenz & Kitai, 1999). Therefore, it appeared that viable reciprocal connectivity between the GABAergic GP and the glutamatergic STN

 DOI: 10.1113/jphysiol.2005.093807

may be sufficient for the generation and recruitment of the STN rebound burst activity (Plenz & Kitai, 1999; Bevan *et al.* 2000) and thus support regenerative oscillatory activity.

Brain slice studies to date have shown that the majority of GP and STN neurones fire single action potentials (Bevan & Wilson, 1999; Cooper & Stanford, 2000) although both GP and STN neurones exhibit anodal break depolarizations upon repolarization of the membrane, which promote rebound firing and, in the case of STN neurones, full-blown bursts. Indeed, intrinsic bursting activity in a proportion of STN cells may be induced by direct manipulation of the membrane potential (Beurrier *et al.* 1999) or more commonly by pharmacological manipulations such as addition of NMDA alone (Zhu *et al.* 2004), TEA-Cl or NMDA plus apamin (Wilson *et al.* 2004*a*). However, the lack of effect of the $GABA_A$ antagonist bicuculline or the glutamate antagonist 6-cyano-7-nitroquinoxaline-2, 3-dione (CNQX) indicated a lack of tonic GABAergic and glutamatergic tone, and this was taken as evidence for a lack of significant functional connectivity between the GP and STN in the rat parasagittal slice preparation (Wilson *et al.* 2004*a*).

It remains possible that a rat parasagittal brain slice containing parts of both the GP and STN may not always preserve sufficiently the connectivity required for functional interaction. Here, by using slices from mouse brain, we have been able effectively to miniaturize the preparation, thereby preserving a greater proportion of the STN–internal capsule–GP axis in the parasagittal plane while still using brain slices of 300 μm (for optimal neuronal visualization and tissue viability). Both the minimal distance between the STN and GP in the sagittal plane ($\sim$ 1.5 mm) and the medio-lateral extent of the STN (1 mm) are reduced by a factor of approximately 0.6 in the mouse, indicating that there may be as much as 50% more functionally interconnected STN–GP tissue in a mouse brain slice than in a rat slice of similar thickness. We demonstrate the functional interconnectivity of GP and STN neurones in this preparation and investigate the role of GABA and glutamate release in shaping and modulating neuronal activity, and consider whether the GP–STN network preserved therein is sufficient for, and capable of, generating regenerative patterns of oscillatory activity, characterized by synchrony and burst firing.

Some of the data has been presented previously in abstract form (Loucif *et al.* 2004).

Methods

In vitro slice preparation

Slices (300 μm thick) were obtained from CB57BL/6JGL male mice (21–40 days old). The age of the animal had no effect on results obtained and therefore all data were pooled. Animals were first anaesthetized with fluorothane and killed by cervical dislocation in accordance with Animals (Scientific Procedures) Act, 1986, UK and the European Communities Council Directive (80/609/EEC). The brain was quickly removed and placed in modified ice-cold artificial cerebral spinal fluid (aCSF) containing (mM): sucrose 208, KCl 2.5, NaH_2PO_4 1.2, $MgCl_2$ 1.3, $MgSO_4$ 8 and glucose 10, buffered to pH 7.4 with $NaHCO_3$ (26 mM), osmolarity between 300 and 310 mosmol l^{-1} and saturated with 95% O_2–5% CO_2.

Using a DTK-1000 Microslicer (Dosaka, Japan) parasagittal slices were cut at a 20 deg angle to the midline in order to maintain the GP, internal capsule and STN as well as parts of the substantia nigra, cortex and striatum. Slices were then transferred to a holding chamber with normal aCSF (where the sucrose (208 mM) had been replaced by NaCl (126 mM)), at room temperature (22–24°C) and thence to a recording chamber at 32–34°C perfused continuously at 2–3 ml min^{-1}.

Biocytin histochemistry

Biocytin tracer studies were initially used to assess reciprocal connectivity between the STN and the GP. Biocytin (Sigma Chemicals, Poole, UK) was mixed with 20% gelatin (Fisher Scientific, Loughborough, UK) in Tris-buffered saline to a final concentration of 50%. Pellets were injected into GP and STN in horizontal (cut 10 deg to true) and parasagittal (cut 20 deg to the midline) sections using either a 1-μl Hamilton syringe or glass pipette attached to a Picospritzer II (General Valve Corporation, NJ, USA) pressure ejection system. A pulse duration of 50 ms at a pressure of 20 psi was routinely used. Following 8–10 h of continuous perfusion with aCSF, slices were fixed in 4% paraformaldeyde in 0.1 M phosphate buffer (PBS) at 4°C for several days. Biocytin was revealed with avidin–biotin complex (Elite ABC kit, Vector Laboratories). After washing in 0.1 M PBS, slices were incubated with 0.3% H_2O_2 for 30 min to block endogenous peroxidase activity. Following further washes in PBS and 0.1% bovine serum albumin, the slices were incubated in sodium borohydride (1% in PBS) for 5 min. Permeabilization in 0.3% Triton X-100 in PBS was followed by incubation with avidin–biotin complex at 4°C overnight. Further washes in PBS were followed by reaction with 3,3′-diaminobenzidine tetrahydrochloride (0.025% DAB), 0.35% ammonium nickel sulphate and 0.0006% H_2O_2 in Tris-HCl (pH 7.4) under visual inspection for 10–40 min. Slices were rinsed and mounted onto gelatine-coated slides. After overnight drying they were dehydrated in alcohol, cleared in xylene and mounted in xylene-based mountant (Eukitt).

Electrophysiological recording

Extracellular recordings were made using borosilicate glass pipettes of resistance 6–10 MΩ filled with 0.9% NaCl. Single units were detected and amplified × 10 000 with Axon Cyberamp 380 and AL402 differential amplifiers (Axon Instruments, Union City, CA, USA). Data acquisition and analysis was performed with a Micro-1401 *mkII* and Spike2 software (Cambridge Electronic Design, UK). Single unit waveforms were discriminated from noise and sorted off-line.

Whole-cell recordings were made using borosilicate glass pipettes of 3- to 6-MΩ resistance containing (mM): potassium gluconate 132, NaCl 8, $MgCl_2$ 2, EGTA 0.5, Hepes 30, GTP 0.3 and Na-ATP 2; adjusted to pH 7.3 with KOH, osmolarity between 290 and 300 mosmol l^{-1}. In some recordings intracellular EGTA (0.5 mM) was replaced by BAPTA (10 mM). Individual neurones were visualized (× 40 water immersion objective) using differential interference contrast infra-red microscopy (Olympus BX 501, Japan) with CCD camera (Hitachi KP-M1, Japan) and contrast enhancement system (ADV-2, Brian Reece Scientific Ltd, Newbury, UK). Membrane currents and potentials were monitored using an Axopatch 200B patch-clamp amplifier (Axon Instruments). All current-clamp recordings were made in Axopatch 200B fast mode and membrane potentials were corrected with respect to the null potential measured at the end of recording. No corrections have been made for the liquid junction potentials, estimated to be +8 mV. Synaptic events were evoked by focal bipolar single shock stimulation (0.2 ms, 1–3 mA) using a constant current stimulation unit (DS2A, Digitimer, UK) placed either within the STN or within the GP.

Drug application

Drugs were applied to the superfusate by exchanging the aCSF for one differing only by the addition of a known concentration of drug after a dead time of approximately 20 s. To determine the effect of drugs, the last 2 min of a 15 min application was analysed. Drugs used were CNQX and DL-2-amino-5-phosphonopentanoic acid (DL-AP5), bicuculline methiodide, picrotoxin (all from Sigma, UK) and *N*-methyl-D-aspartate (NMDA) and apamin (from Tocris, UK).

Analysis

Burst and oscillatory activity was analysed using the program of Kaneoke & Vitek (1996). The burst detection algorithm was used to identify cells firing in patterns that differed significantly from the Poisson distribution with a mean of 2, thus giving a burst index > 0.5. Only cells with a burst index > 0.5, firing three or more bursts in the 2-min analysis period and having a significant oscillation below 3 Hz were considered burst firing. The Lomb periodogram (power spectrum) was used to determine the frequency of any significant oscillation ($P < 0.05$) while patterns of the bursting mode were described by burst frequency, mean number of spikes per burst and the mean interspike interval (ISI) within bursts.

All numerical data are expressed as mean and standard error unless otherwise stated.

Results

Anatomical interconnectivity between the GP and STN

In order to assess the anatomical connectivity between the GP and STN in two different slice orientations, we exploited the retrograde and anterograde transport of the neuroanatomical tracer biocytin. Injections of biocytin into the STN were made in eight horizontal slices using a Hamilton syringe. However, biocytin was seen to spread from the STN in only one slice, labelling the internal capsule. Nine horizontal slices were injected with biocytin in the GP using a Hamilton syringe and once again in only one case were labelled fibres observed traversing to the STN.

In order to produce a more discrete injection of biocytin and prevent extensive damage to the slice, pressure injections from a glass micropipette were made. Five horizontal slices were thus injected with biocytin into the STN. In two slices there was no spread of biocytin from the nucleus, while in the remaining three slices labelled fibres were observed heading from the STN towards the GP and striatum. Of the seven horizontal slices in which biocytin that were successfully pressure injected and revealed in the GP, six showed good labelling of fibres in the internal capsule towards the STN.

Biocytin injections were made into the STN in eight parasagittal slices using a Hamilton syringe. In all eight slices, reaction product was observed labelling fibres which funnelled towards the GP (see Fig. 1*C* and *D*). Labelled cell bodies were observed in all cases. Injections by Hamilton syringe into the GP were carried out in nine slices. In all cases extensive labelling from the GP to STN was evident. All six parasagittal slices that were pressure-injected with biocytin in the STN showed strong labelling of STN and evidence of fibres coursing towards the GP, and diffuse labelling of the GP itself. Pressure-injection of biocytin into the GP was carried out in 10 parasagittal slices which showed strong labelling of injection sites and fibres heading towards the STN and further caudally to the substantia nigra pars reticulata (see Fig. 1*A* and *B*).

Thus, although axonal labelling between the GP and STN was observed in both planes of section, the most robust connectivity, including labelling of axonal tracts

and cell bodies, was observed in 20 deg parasagittal sections. This plane of section was used for all subsequent electrophysiological recordings.

Synaptic interconnectivity between the GP and the STN

Whole-cell recordings in one region, together with electrical stimulation in the other were used to show functional connectivity between the GP and the STN. Neurones were considered viable if resting membrane potential (voltage at steady state current of 0) was more negative than −40 mV, input resistance greater than 100 MΩ and action potential amplitude greater than 50 mV. Neurones that did not meet these criteria were discarded.

The majority of GP cells recorded (> 90%) corresponded to type A neurones of the rat (Cooper & Stanford, 2000), the type II cells of guinea-pig (Nambu & Llinás, 1994) and the *in vivo* bursting cells of the rat (Kita & Kitai, 1991). They were easily identified by the presence of a time- and voltage-dependent 'sag' of membrane potential evoked by hyperpolarizing current steps indicative of the anomalous inward rectifier, I_h, and anodal break rebound depolarizations, which were often accompanied by action potential firing (Cooper & Stanford, 2000) (see Fig. 2*A*). All STN cells displayed both I_h and rebound depolarizations (Fig. 2*B*), which are characteristic features of STN neurones (Nakanishi *et al.* 1987; Bevan *et al.* 2000, 2002; Wigmore & Lacey, 2000).

As there is little anatomical evidence for another GABA projection to the STN (other than the GP) and glutamate projection to the GP (other than the STN) which courses through the STN, we used single-shock electrical stimulation to evoke excitatory and inhibitory postsynaptic potentials in the GP and STN, respectively. Connectivity was assumed if the evoked synaptic current responses were > 20 pA and thus clearly observed above the noise, which was routinely < 15 pA at a holding potential of −50 mV. Using these criteria, stimulation of the STN evoked bicuculline-resistant EPSCs in the GP in 22 of 33 slices (66%), which were blocked by the glutamate antagonists CNQX (10 μM) and DL-AP5 (100 μM, $n = 5$, Fig. 2*A*). Often responses with double peaks were observed (Fig. 2) that could be due to activation of polysynaptic circuitry or promotion of a somatic spike, which may evoke further transmitter release.

Postsynaptic responses mixed with antidromic spikes with a spike width around 1 ms, evoked as a consequence

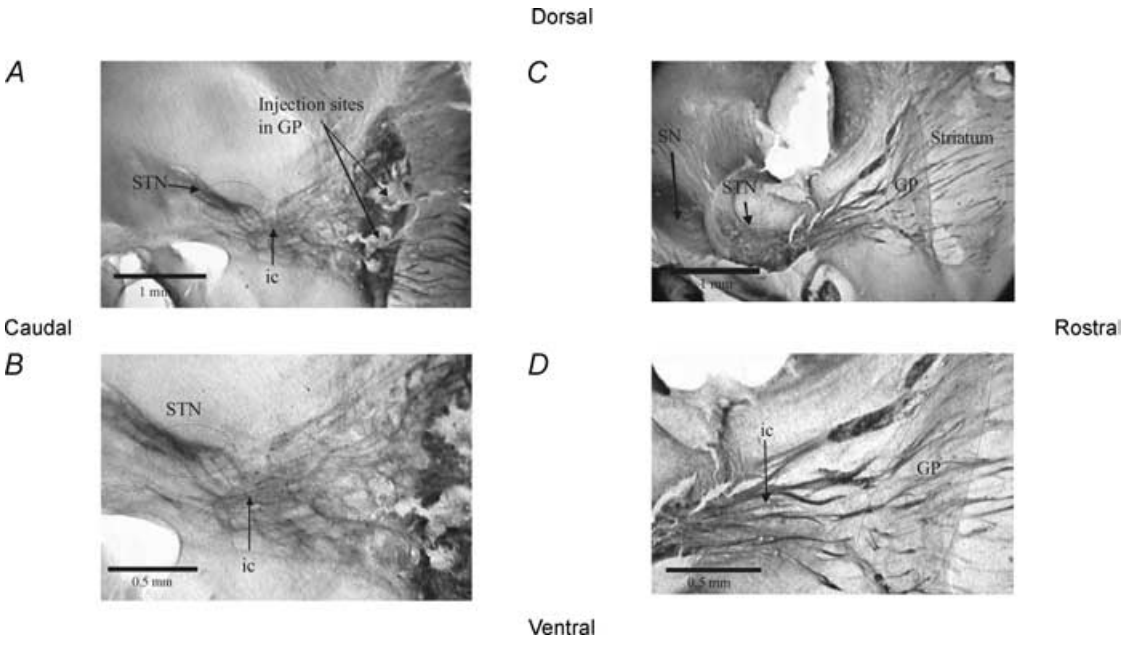

Figure 1. Parasagittal slices in which the GP and the STN have been injected with biocytin
A, a parasagittal slice from the mouse brain in which the GP has been injected with biocytin. Labelled fibres can be seen heading from the GP in both directions; into the striatum, and funnelling down towards the STN, and travelling beyond the STN. *B*, close-up of the GP showing the labelled fibres funnelling towards the STN, through the internal capsule and through the STN. *C*, photograph of parasagittal mouse brain slice in which the STN has been injected with biocytin. Labelled fibre tracts heading towards the GP and striatum can be seen clearly, as can labelling in the SN. *D*, close-up of the labelled fibre tracts in this slice heading from the STN to the GP. The GP can be distinguished at this power as a region of diffuse labelling, possibly as a result of anterograde labelling of terminals of fibres of STN origin. STN, subthalamic nucleus; GP, globus pallidus; ic, internal capsule; SN, substantia nigra.

of stimulation of efferent axons and indicative of reciprocal connectivity, were occasionally observed. These large action currents often masked the postsynaptic response and were therefore avoided by changing the location of stimulation and reducing stimulation amplitude.

Stimulation of the GP in the presence of CNQX (10 μM) and DL-AP-5 (100 μM) evoked $GABA_A$ receptor-mediated IPSCs in the STN in 44/59 slices (75%) which reversed at −64 mV, close to the theoretical equilibrium potential for chloride and were blocked by the $GABA_A$ antagonist bicuculline (10 μM, $n = 7$, Fig. 2*B*). In 2/2 slices, stimulation of the GP evoked responses in the STN while subsequent stimulation of the STN evoked responses in the GP, indicative of reciprocal connectivity.

Evidence for spontaneous (action potential-dependent and independent) release of GABA and glutamate on both GP and STN cells was observed. In STN cells at a holding potential of −50 mV, spontaneous outward currents indicative of sIPSCs were observed in 85/150 (57%) cells while inward currents indicative of sEPSCs were observed in 106/150 cells (71%). Indeed inward and outward currents were often observed in the same recording (see Fig. 3 at potentials less than −50 mV). In GP cells, EPSCs were observed in 26/43 cells (61%) while IPSCs were observed in all 43 cells recorded.

The postulated mechanism allowing regenerative oscillatory activity, in the isolated GP–STN network, involves GABA-induced rebound depolarizations with accompanying action potential firing of STN neurones (Plenz & Kitai, 1999; Bevan *et al.* 2000). We set out to replicate these responses in our mouse slice preparation. Firstly STN-evoked EPSPs were shown to be able to trigger action potentials in the GP ($n = 3$, Fig. 4*A*). In addition, single shock simulation in the GP evoked a single IPSP in the STN. By increasing the number of shocks, IPSPs were observed to summate and produce rebound depolarizations, sufficient to promote action potential firing (Fig. 4*B*, × 5 and × 10 stimulations). Summated IPSPs were also able to inhibit STN action potential firing, while the following rebound depolarizations were able to elicit further action potential firing ($n = 4$, Fig. 4*C*). Thus, in our mouse slice preparation, as in other preparations, it appears that we have a potential mechanism for the promotion of reverberating oscillatory activity.

Spike firing patterns in STN are independent of ongoing GABA or glutamate release

Does the connectivity and GABA release from the GP play a role in the rate and pattern of spontaneous STN activity in the mouse slice preparation? To address this question we used extracellular single unit recordings of STN activity and bath application of the $GABA_A$ antagonist picrotoxin

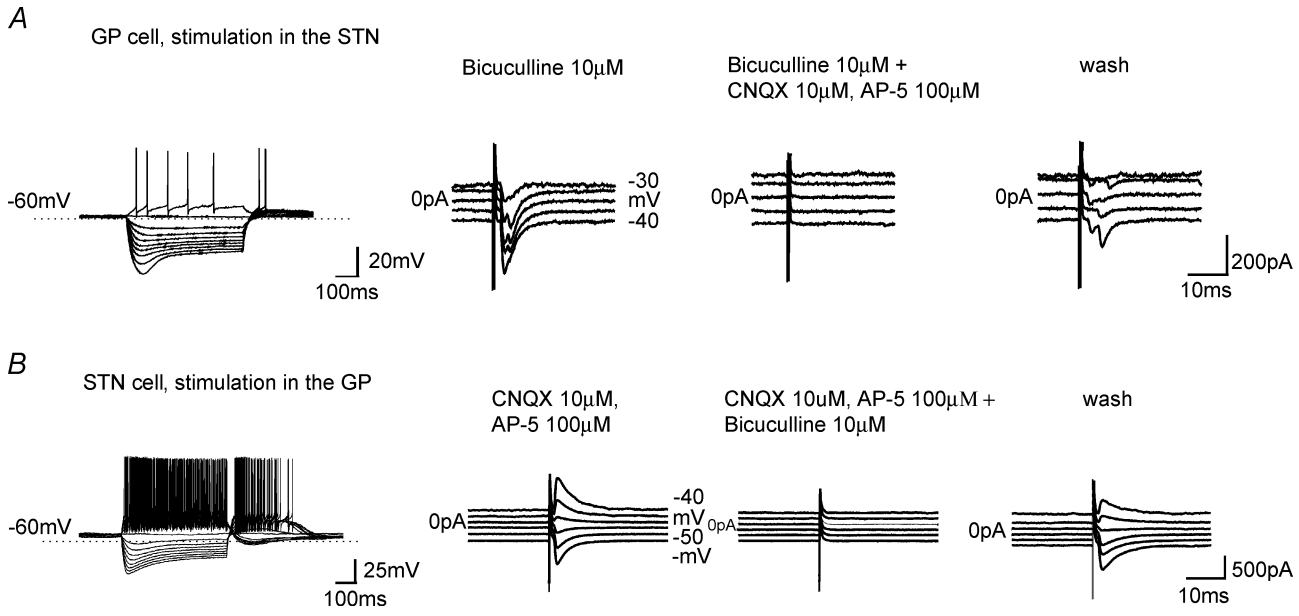

Figure 2. GP–STN connectivity established by evoked synaptic currents
Typical electrophysiological characteristics of type A GP cell (*A*) and STN cell (*B*). Records of membrane potential from a GP and STN cell in response to current steps (25-pA increments) from resting membrane potential. Note I_h and the extensive rebound burst of action potentials on repolarization of the membrane. *A*, current responses to single shock electrical stimulation in the STN at holding potential from −30 to −70 mV promotes inward currents, which are reversibly blocked by the glutamate antagonists CNQX and AP-5. *B*, current responses to single shock electrical stimulation in the GP at holding potential from −40 to −90 mV promote inward and outward currents that reverse polarity at −65 mV, which are reversibly blocked by the $GABA_A$ receptor antagonist bicuculline.

(50 μM) in order to eliminate any effects of synaptically released GABA.

In control slices, 74/76 (97%) STN cells fired tonically at a rate of 10.3 ± 1.3 Hz. The remaining two cells exhibited burst-firing characteristics. Application of picrotoxin resulted in no effect on the frequency of all nine (non-bursting) STN cells tested indicating that at least under control conditions the tonic release of GABA has no effect on firing rate.

To block any glutamatergic tone the glutamate antagonist CNQX (10 μM) was applied. No change of firing rate was observed in eight (non-bursting) STN cells indicating that at least under control conditions the tonic release of glutamate has no effect on firing rate.

NMDA and apamin-induced burst firing in the STN is also independent of glutamate and GABA release

In an attempt to replicate the bursting activity observed in STN neurones during dopamine depletion *in vivo* and increase the activity of GP cells and thus promote GABA release, the ionotropic glutamate receptor agonist NMDA (20 μM) was bath applied. This induced an increase in firing rate of $415 \pm 103\%$ ($n = 15$). In 3/18 STN cells (17%) application of NMDA (20 μM) changed the firing pattern from a regular to a burst-firing pattern. However, STN bursting activity was much more reproducible if NMDA (20 μM) was applied in conjunction with the calcium-activated potassium channel blocker, apamin (20–100 nM). Addition of 20 nM apamin induced bursting in 5/19 STN cells (26%), while 50 nM apamin induced bursting in 12/25 cells (48%), and 100 nM apamin in 17/33 cells (52%). All STN bursting activity appeared calcium dependent as dialysis with internal solutions containing the calcium chelator BAPTA (10 mM, $n = 6$) abolished all spiking activity within 15 min following breakthrough. All burst activity was therefore recorded with intracellular solutions containing EGTA (0.5 mM).

The burst parameters of 25 STN cells were analysed using the program of Kaneoke & Vitek (1996) (see Fig. 5). Once bursting had been induced, bursting parameters appeared independent of the applied apamin concentration and therefore all data were pooled. Analysis revealed a slow oscillatory burst at a frequency of 0.46 ± 0.06 Hz, each burst containing 31.7 ± 5.4 spikes, with an ISI within bursts of 24.2 ± 3.7 ms.

Although, probably intrinsic in nature (see Wilson *et al.* 2004*a*), such bursting activity would be expected to promote increased GABA or glutamate release in the STN and GP, respectively. (Indeed, 6/12 single-unit recordings from GP cells show NMDA/apamin-induced burst firing, see Fig. 7).

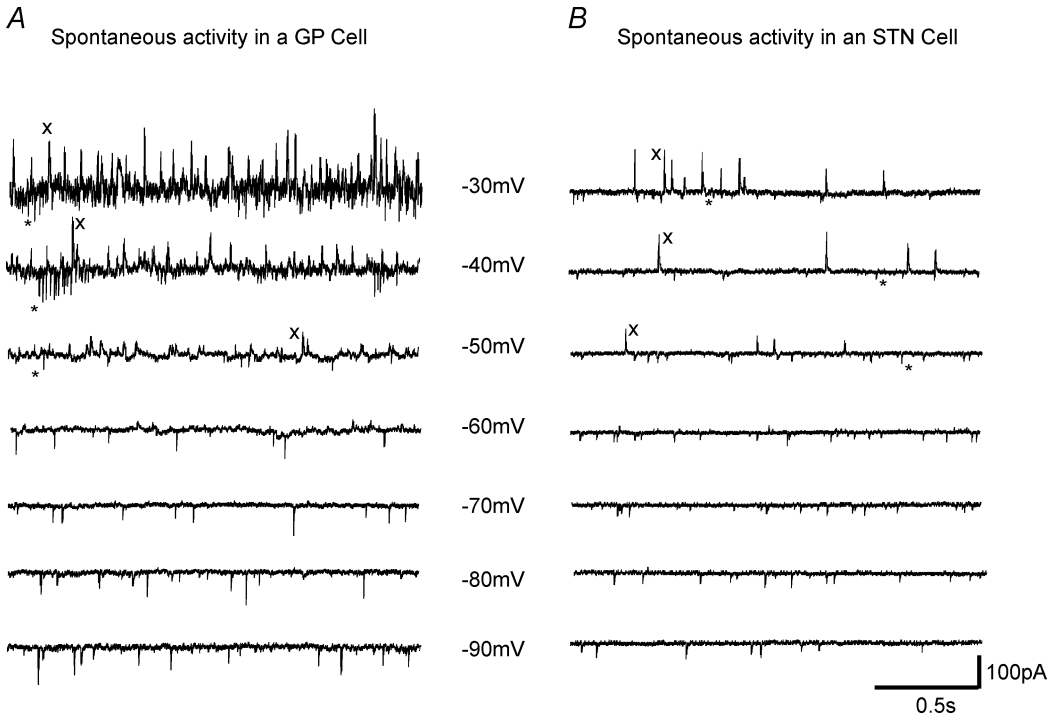

Figure 3. Spontaneous synaptic currents showing functional neurotransmitter release
Spontaneous inward and outward synaptic currents recorded from a GP cell (*A*) and an STN cell (*B*) at holding potentials −30 to −90 mV. In both GP and STN cells, note the fast inward currents (*) recorded at potentials more depolarized than −50 mV indicative of sEPSCs and outward currents (x) observed at potentials depolarized to −60 mV indicative of sIPSCs.

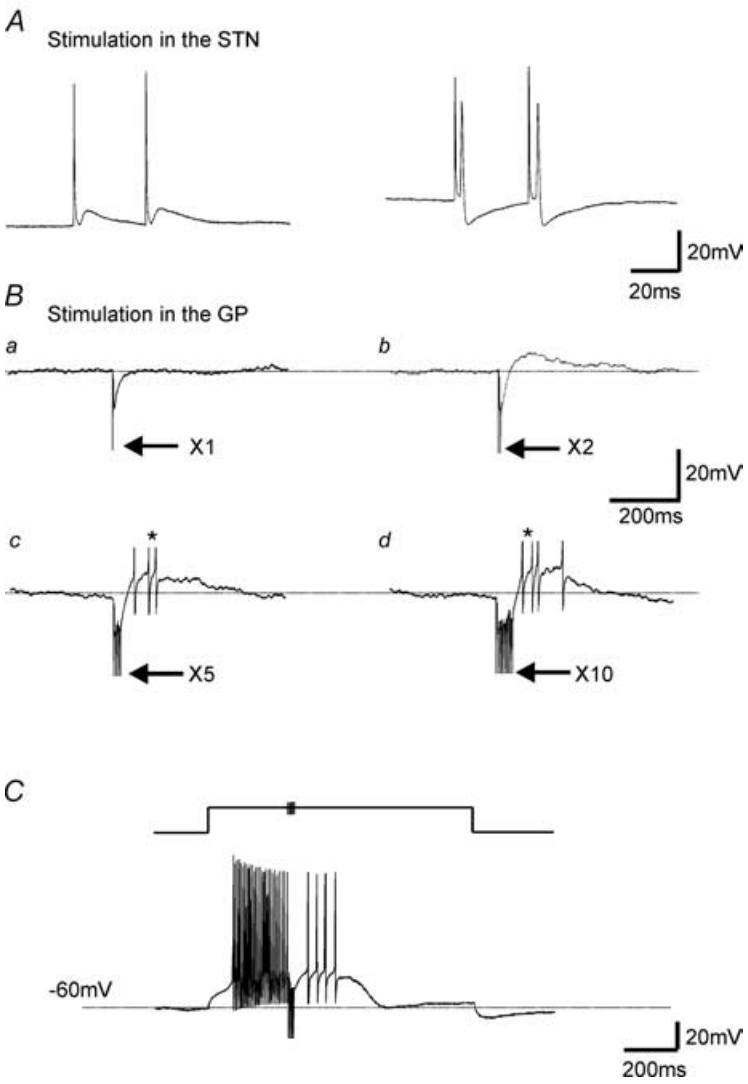

Figure 4. Rebound depolarizations in STN: the postulated mechanism for regenerative oscillations are present
A, records of membrane voltage from a GP cell in response to single-shock stimulation in the STN, which is able to promote an EPSP and action potential firing. *B*, current-clamp recordings from an STN neurone held at −50 mV. Single-shock electrical stimulation of the GP evoked a single IPSP (*i*). Double-shock electrical stimulation at interpulse interval of 5 ms evoked IPSP and small rebound depolarizations (*ii*). This rebound depolarization is able to promote action potential firing upon × 5 (*iii*) and × 10 (*iv*) stimulation (at 200 Hz). Arrows denote electrical stimulation artefacts; * denotes truncated action potentials. *C*, voltage record from a cell held at −60 mV. A 1000-ms duration, 0.1-nA step depolarization promoted fast action potential firing. During the depolarizing step, five stimulations in the GP at 200 Hz evoked IPSPs that summated and blocked action potential firing. Following this inhibition there was a rebound depolarization, which was able to promote further action potential firing albeit at a low rate.

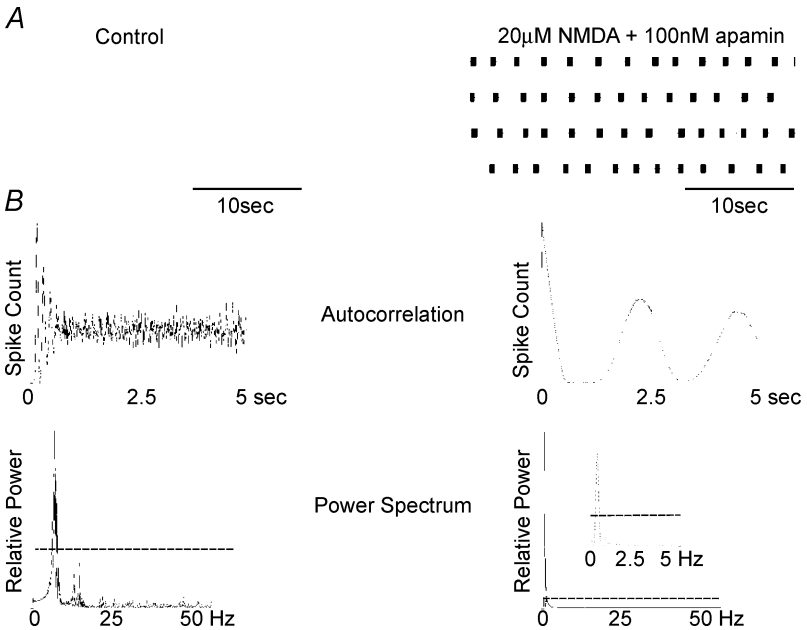

Figure 5. NMDA and apamin induced burst firing in STN cells
Wavemark data collated from extracellular single-unit recording from a spontaneously firing STN neurone. *A*, continuous 2-min records of action potential firing in control and following perfusion with NMDA (20 μM) and apamin (100 nM). The autocorrelogram and associated Lomb power spectrum are shown in *B*. Dashed line indicates a significance level of $P < 0.05$. In control conditions, tonic firing was observed at a rate of 6.2 Hz while NMDA and apamin induced bursting at 0.4 Hz.

Thus, any modulatory effect of GABA (from the GP) and glutamate release (possibly from axon collaterals from the STN and cortex) on the firing frequency and pattern of activity should be enhanced and clearly evident when abolished by addition of antagonists. However, this was not the case. Using the whole-cell technique, picrotoxin (50 μM) was applied to five NMDA/apamin-induced bursting cells, which all continued to burst fire with no significant change in oscillation frequency ($P = 0.86$), spikes per burst ($P = 0.86$), or ISI within bursts ($P = 0.5$) (Fig. 6*B*). CNQX (100 μM) was added to five bursting cells. All cells continued to burst fire with no significant change in oscillation frequency ($P = 0.31$), spikes per burst ($P = 0.81$), or ISI within bursts ($P = 0.19$) (Fig. 6*A*). Thus, despite 75% of our GP cells being connected to the STN and 66% of STN cells being connected to the GP, and extensive evidence for spontaneous IPSCs and EPSCs in our mouse slice preparation, we have no evidence that GABA or glutamate has any role in promoting, shaping or modulating the NMDA/apamin-induced burst-firing patterns in STN neurones.

Single-unit recordings of neuronal activity were made from a number of cells simultaneously in the STN and the GP. Seven pairs of regular-firing STN–GP neurones were recorded. In the presence of NMDA (20 μM) and apamin (100 nM), bursting of both cells was observed in 3/7 pairs (Fig. 7*A*). In three pairs, only the STN exhibited bursting activity (Fig. 7*B*) and in one pair bursting was promoted only in the GP unit. In all cases the activity observed remained totally uncorrelated. Six pairs of bursting STN neurones were also recorded. In each pair, the regular/tonic activity in control conditions was uncorrelated as was the bursting activity induced by application of NMDA (20 μM) and apamin (100 nM) (Fig. 7*C*).

Discussion

The mouse slice preparation

Using an organotypic culture preparation, Plenz & Kitai (1999) proposed that the isolated GP and STN constitute a central pacemaker responsible for oscillatory activity; that is, recurrent excitation of inhibitory GP cells forming a feedback loop which is able to maintain synchronized burst discharges. However, *in vivo* experiments have indicated that rhythmic activity in STN–GP neurones is driven by the cortex (Magill *et al.* 2000), with dopamine depletion rendering the system more sensitive to rhythmical cortical input (Magill *et al.* 2001). Thus, apart from the culture

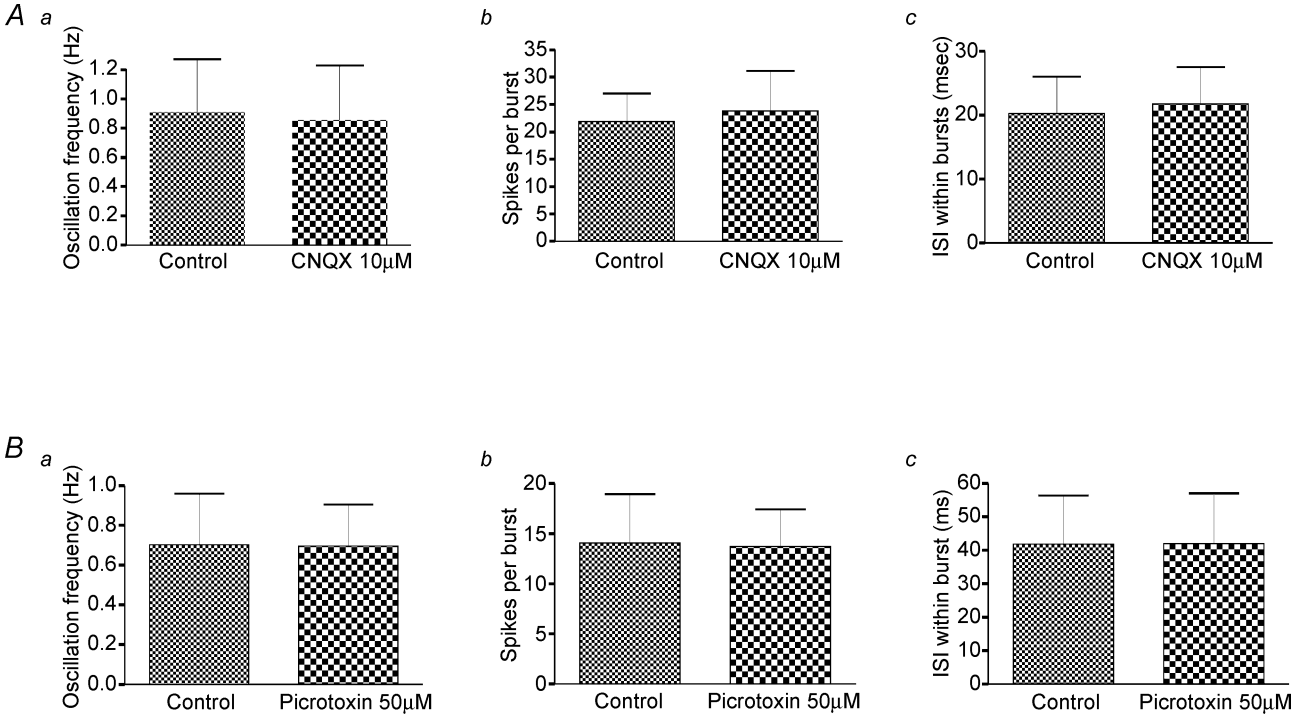

Figure 6. Bursting is independent of glutamate or GABA release
A, data pooled from five different STN cells indicate that bath application of the glutamate receptor antagonist CNQX (10 μM) had no effect on the oscillation frequency (*i*), number of spikes per burst (*ii*) or the interspike interval within bursts (*iii*). *B*, data pooled from five STN cells indicate that the $GABA_A$ receptor antagonist picrotoxin (50 μM) had no effect on the oscillation frequency (*i*), number of spikes per burst (*ii*) or the interspike interval (ISI) within bursts (*iii*).

preparation is there evidence that the isolated GP and STN can maintain regenerative oscillatory activity?

To date, few studies have used the slice preparation to directly investigate the cellular mechanisms by which patterned activity arises. Here, we have used morphological and electrophysiological techniques to show that a mouse parasagittal slice cut 20 deg to the midline maintains functional interconnectivity between the GP and the STN. We then used this model to directly investigate the role of GABA and glutamate release in shaping and modulating GP and STN neuronal activity.

In our interconnected mouse preparation, the majority of STN cells (97%) show single spiking activity, and although spontaneous IPSCs (indicating connectivity from the GP) were observed, this activity was unaffected by bath application of picrotoxin showing that this tonic release of GABA is insufficient to have functional consequences. Indeed, in rat brain slices, the majority (68%) of GP cells are quiescent or fire at a low regular rate (< 8 Hz) (Cooper & Stanford, 2000). Thus, if the GP cells in our mouse slice preparation show similar properties, one might expect GABA tone in the unstimulated STN to be low.

Numerous spontaneous EPSCs were observed in STN neurones, indicating glutamatergic tone. As the presence of intrinsic axon collaterals within the STN (Kita *et al.* 1983) has not been confirmed (Hammond & Yelnik, 1983; Sato *et al.* 2000; Wilson *et al.* 2004*a*), these sEPSCs probably arise from extrinsic sources such as the thalamus, pedunculopontine nucleus or cortex. However, the addition of CNQX and block of the tonic glutamatergic tone mediated by spontaneous EPSCs *in vitro*, proved insufficient to affect the rate or pattern of STN cell firing.

Inducing bursting activity

A pharmacological model of burst firing was sought not only to mimic the activity observed in dopamine-depleted animals, but also as an attempt to increase spontaneous and phasic GABA and glutamate release in the connected GP–STN network. Indeed, bursting activity not only facilitates neurotransmitter release but can also play a role in synaptic plasticity and lead to dynamic changes in synaptic physiology (Lisman, 1997).

Application of NMDA alone has recently been reported to promote burst firing in STN neurones (Zhu *et al.* 2004), although this was not a robust model of burst firing in our hands and required the co-application of apamin (20–100 nM). Apamin has previously been shown to enhance NMDA-mediated burst firing, both in

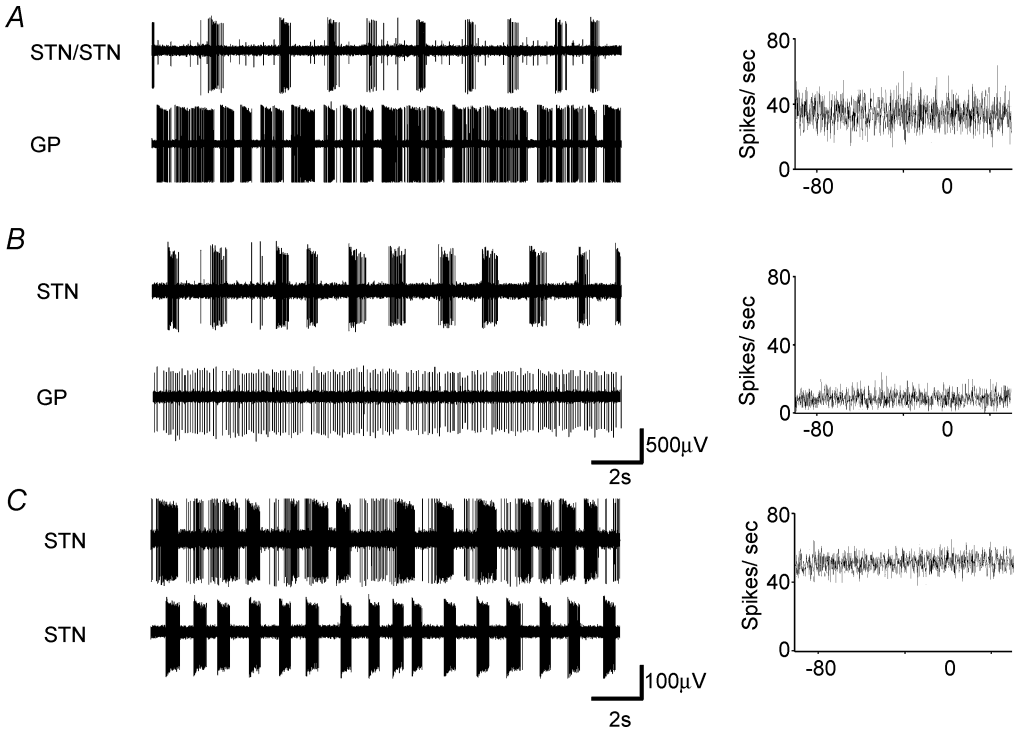

Figure 7. Parallel recordings in the STN and GP show uncorrelated activity
Simultaneous single-unit recordings from STN and GP neurones in the presence of NMDA (20 μM) and apamin (100 nM). *A*, a bursting STN cell and a bursting GP cell, with the associated cross-correlation. Note the presence of a second non-bursting unit within the STN recording. *B*, a bursting STN cell and a regular firing GP cell, and the associated cross-correlation *C*, two STN bursting units and the associated cross-correlation.

dopaminergic neurones (Seutin *et al.* 1993) and in the rat STN (Wilson *et al.* 2004*a*). Other pharmacological agents that can enhance the propensity to burst through the modulation of apamin-sensitive Ca^{2+}-activated K^+ channels (SK, $Ca_v2.2$) include TEA-Cl (Wilson *et al.* 2004*a*), bicuculline methiodide (Johnson & Seutin, 1997) and the mGluR agonist 1S,3R ACPD (Beurrier *et al.* 1999). Indeed, 1S,3R ACPD (100–200 μM) can produce burst firing of STN cells but does not appear a robust finding (Wilson *et al.* 2004*a*; K. Loucif, unpublished observations).

A lack of evidence for a functional role of the GP in NMDA/apamin-induced bursting

As burst firing induces the release of more transmitter than single spiking (Lisman, 1997), and STN cells display a reverse spike frequency adaptation and a steep secondary range in their frequency–intensity curves (Wilson *et al.* 2004*b*) and are therefore more sensitive to synaptic input when excited in the burst range, we expected to observe more pronounced effects of picrotoxin and CNQX application in our model of bursting. However, applications of GABA or glutamate antagonists appear to have little effect on the bursting parameters. Thus, despite 66% of STN cells being connected to the GP and 75% of our GP cells being connected to the STN (which may promote rebound depolarization and action potential firing, see Fig. 4), we have no evidence that GABA or glutamate release has any role in promoting, shaping or modulating NMDA/apamin-induced burst firing patterns in STN neurones.

The GP–STN network: why no oscillations?

The mechanism by which reverberating oscillatory activity arises between the GP and STN is thought to involve a hyperpolarization-induced rebound depolarization driving GP neuronal activity and subsequent GABA release from terminals with the STN. Indirect evidence for this scenario emanates from the observed bursting activity promoted on membrane hyperpolarization (Beurrier *et al.* 1999), the voltage-dependent generation of plateau potentials (Otsuka *et al.* 2001), organotypic cultures which can sustain reverberating bursting activity through interplay of the STN and GP (Plenz & Kitai, 1999) and the results of Bevan *et al.* (2000) and those presented here in Fig. 4 which imply that GABA release from the GP can induce rebound depolarizations in the STN.

Therefore, it was surprising that in this mouse preparation, in which there is reciprocal connectivity between the STN and the GP, there was no increase in oscillatory bursting activity was found in the control slices, and that GABA and glutamate appear to have little effect on shaping the pattern of burst firing induced by pharmacological interventions. Indeed, if GABA and glutamate were a fundamental, prerequisite for bursting in this network, the addition of antagonists should have curtailed the entire oscillation.

Although we are confident of preservation of reciprocal connectivity between the GP and STN, we cannot rule out the possibility that preservation of other anatomical connections (such as cortical and striatal inputs) is required for a functional network or may play a role in sculpting network activity. Indeed, as already stated, the driving force of the STN and GP network may well be the cortex itself (Magill *et al.* 2000), while increased synchronized striatal output, which has been reported in 6-hydroxydopamine-lesioned animals (Tseng *et al.* 2001), may enhance correlated oscillatory activity in the GP–STN network (Terman *et al.* 2002).

A second, but not necessarily alternative reason for the lack of oscillatory firing in this isolated preparation could be because the tissue was not taken from dopamine-depleted animals. Indeed, the extent of dopamine depletion (if any) in our slices is unknown, but adaptive changes, not necessarily confined to the STN and GP, caused by chronic dopamine depletion appear a fundamental requirement for instigating the large-scale oscillatory basal ganglia activity seen in animal models of Parkinson's disease. Such adaptive changes, perhaps by modification of striato-pallidal (Tseng *et al.* 2001) or cortico-subthalamic pathways (Magill *et al.* 2001) and also of STN function (Zhu *et al.* 2002; Tofighy *et al.* 2003), may be necessary in promoting burst-firing in our slice preparation.

In conclusion, the *in vitro* mouse slice preparation in which there is functional GP–STN connectivity, does not produce STN neuronal bursting activity without pharmacological interventions, and when induced to burst does not require GABA or glutamate release to maintain the activity. Thus, we have no evidence that the isolated GP–STN network in the mouse slice preparation can act as a pacemaker for regenerative oscillatory activity in the basal ganglia.

References

Albin RL, Young AB & Penney JB (1989). The functional anatomy of basal ganglia disorders. *Trends Neurosci* **12**, 366–375.

Bergman H, Wichmann T, Karmon B & Delong MR (1994). The primate subthalamic nucleus. II. Neuronal activity in the MPTP model of parkinsonism. *J Neurophysiol* **72**, 507–520.

Beurrier C, Congar P, Bioulac B & Hammond C (1999). Subthalamic nucleus neurones switch from single-spike activity to burst-firing mode. *J Neurosci* **19**, 599–609.

Bevan MD, Magill PJ, Hallworth NE, Bolam JP & Wilson CJ (2002). Regulation of the timing and pattern of action potential generation in rat subthalamic neurones *in vitro* by GABA-A IPSPs. *J Neurophysiol* **87**, 1348–1362.

Bevan MD & Wilson CJ (1999). Mechanisms underlying spontaneous oscillation and rhythmic firing in rat subthalamic neurones. *J Neurosci* **19**, 7617–7628.

Bevan MD, Wilson CJ, Bolam JP & Magill PJ (2000). Equilibrium potential of $GABA_A$ current and implications for rebound burst firing in rat subthalamic neurones *in vitro*. *J Neurophysiol* **83**, 3169–3172.

Cooper AJ & Stanford IM (2000). Electrophysiological and morphological characteristics of three subtypes of rat globus pallidus neuron *in vitro*. *J Physiol* **527**, 291–304.

DeLong M (1990). Primate models of movement disorders of basal ganglia origin. *Trends Neurosci* **13**, 281–285.

Filion M & Tremblay L (1991). Abnormal spontaneous activity of globus pallidus neurones in monkeys with MPTP-induced parkinsonism. *Brain Res* **547**, 142–151.

Hammond C & Yelnik J (1983). Intracellular labelling of rat subthalamic neurones with horseradish peroxidase: computer analysis of dendrites and characterization of axon arborization. *Neuroscience* **8**, 781–790.

Heimer G, Bar-Gad I, Goldberg JA & Bergman H (2002). Dopamine replecament therapy reverses abnormal synchronization of pallidal neurones in the 1-methyl-4-phenyl-1,2,3,6-tetrahydropyridine primate model of Parkinsonism. *J Neurosci* **22**, 7850–7855.

Johnson SW & Seutin V (1997). Bicuculline methiodide potentiates NMDA-dependent burst firing in rat dopamine neurones by blocking apamin-sensitive Ca^{2+}-activated K^+ currents. *Neurosci Lett* **231**, 13–16.

Kaneoke Y & Vitek JL (1996). Burst and oscillation as disparate neuronal properties. *J Neurosci Methods* **68**, 211–223.

Kita H, Chang HT & Kitai ST (1983). The morphology of intracellularly labelled rat subthalamic neurones: a light microscopic analysis. *J Comp Neurol* **215**, 245–257.

Kita H & Kitai ST (1991). Intracellular study of rat globus pallidus neurones: membrane properties and responses to neostriatal, subthalamic and nigral stimulation. *Brain Res* **564**, 296–305.

Levy R, Ashby P, Hutchinson WD, Lang AE, Lozano AM & Dostrovsky JO (2002). Dependence of subthalamic nucleus oscillations on movement and dopamine in Parkinson's disease. *Brain* **125**, 1196–1209.

Lisman JE (1997). Bursts as a unit of neural information: making unreliable synapses reliable. *Trends Neurosci* **20**, 38–43.

Loucif KC, Wilson CL, Lacey MG & Stanford IM (2004). Functional connectivity between the globus pallidus and subthalamic nucleus in a mouse brain slice preparation. *J Physiol* **555.P**, PC29.

Magill PJ, Bolam JP & Bevan MD (2000). Relationship of activity in the subthalamic nucleus-globus pallidus network to cortical electroencephalogram. *J Neurosci* **20**, 820–833.

Magill PJ, Bolam JP & Bevan MD (2001). Dopamine regulates the impact of the cerebral cortex on the subthalamic nucleus-globus pallidus network. *Neuroscience* **106**, 313–330.

Magnin M, Morel A & Jeanmonod D (2002). Single unit analysis of the pallidum, thalamus, and subthalamic nucleus in Parkinsonian patients. *Neuroscience* **96**, 549–564.

Nakanishi H, Kita H & Kitai ST (1987). Electrical membrane properties of rat subthalamic neurones in an in vitro slice preparation. *Brain Res* **437**, 35–44.

Nambu A & Llinás R (1994). Electrophysiology of globus pallidus neurones *in vitro*. *J Neurophysiol* **72**, 1127–1139.

Otsuka T, Murakami F & Song WJ (2001). Excitatory postsynaptic potentials trigger a plateau potential in rat subthalamic neurones at hyperpolarised states. *J Neurophysiol* **86**, 1816–1825.

Plenz D & Kitai ST (1999). A basal ganglia pacemaker formed by the subthalamic nucleus and external globus pallidus. *Nature* **400**, 677–682.

Sato F, Parent M, Levesque M & Parent A (2000). Axonal branching pattern of neurones of the subthalamic nucleus in primates. *J Comp Neurol* **424**, 142–152.

Seutin V, Johnson SW & North RA (1993). Apamin increases NMDA-induced burst-firing of rat mesencephalic dopamine neurones. *Brain Res* **630**, 341–344.

Terman D, Rubin JE, Yew AC & Wilson CJ (2002). Activity patterns in a model for the subthalamopallidal network of the basal ganglia. *J Neurosci* **22**, 2963–2976.

Tofighy A, Abbott A, Centonze D, Cooper AJ, Noor E, Pearce SM, Puntis M, Stanford IM, Wigmore MA & Lacey MG (2003). Excitation by dopamine of rat subthalamic nucleus neurones *in vitro*-a direct action with unconventional pharmacology. *Neuroscience* **116**, 157–166.

Tseng KY, Kaseanetz F, Kargieman L, Riquelme LA & Murer MG (2001). Cortical slow oscillatory activity is reflected in the membrane potential and spike trains of striatal neurones in rats with chronic nigrostriatal lesions. *J Neurosci* **21**, 6430–6439.

Wigmore MA & Lacey MG (2000). Kv3-like persistent, outwardly rectifying, Cs^+ permeable, K^+ current in rat subthalamic nucleus neurones. *J Physiol* **527**, 493–506.

Wilson CL, Puntis M & Lacey MG (2004*a*). Overwhelmingly asynchronous firing of rat subthalamic nucleus neurones in brain slices provides little evidence for intrinsic connectivity. *Neuroscience* **123**, 187–200.

Wilson CJ, Weyrick A, Terman D, Hallworth NE & Bevan MD (2004*b*). A model of reverse spike frequency adaptation and repetitive firing of subthalamic nucleus neurones. *J Neurophysiol* **91**, 1963–1980.

Zhu ZT, Munhall A, Shen KZ & Johnson SW (2004). Calcium-dependent subthreshold oscillations determine bursting activity induced by N-methyl-D-aspartate in rat subthalamic neurones *in vitro*. *Eur J Neurosci* **19**, 1296–1304.

Zhu ZT, Shen KZ & Johnson SW (2002). Pharmacological identification of inward current evoked by dopamine in rat subthalamic neurones *in vitro*. *Neuropharmacology* **42**, 772–781.

Acknowledgements

This study was supported by The Wellcome Trust project grant 068818, The Parkinson's Disease Society, a research grant from the Royal Society (I.M.S.) and a Research Leave Fellowship 063461 (M.G.L.). I.M.S. is a Medical Research Council (MRC) Career Establishment Fellow.